Selectivity Determinants of Inhibitor Binding to Human 20α-Hydroxysteroid Dehydrogenase: Crystal Structure of the Enzyme in Ternary Complex with Coenzyme and the Potent Inhibitor 3,5-Dichlorosalicylic Acid†

Urmi Dhagat,[||,‡] Satoshi Endo,[§,||] Rie Sumii,[§] Akira Hara,[§] and Ossama El-Kabbani*[,‡]

Medicinal Chemistry and Drug Action, Monash Institute of Pharmaceutical Sciences, 381 Royal Parade, Parkville, Victoria 3052, Australia, Laboratory of Biochemistry, Gifu Pharmaceutical University, Mitahora-higashi, Gifu 502-8585, Japan

Received March 30, 2008

The crystal structure of human 20α-hydroxysteroid dehydrogenase (AKR1C1) in ternary complex with the coenzyme $NADP^+$ and the potent inhibitor 3,5-dichlorosalicylic acid was determined at a resolution of 1.8 Å. The inhibitor is held in place by a network of hydrogen bonding interactions with the active site residues Tyr55, His117, and His222. The important role of the nonconserved residues Leu54, His222, Leu306, and Leu308 in inhibitor binding and selectivity was determined by site-directed mutagenesis.

Introduction

Hydroxysteroid dehydrogenases (HSDs)[a] play a pivotal role in the prereceptor regulation of the concentration of active steroid hormones.[1,2] The enzymes belong to two protein superfamilies, the aldo-keto reductase (AKR)[3] superfamily and the short-chain dehydrogenase/reductase[4] superfamily. There are four human HSDs belonging to the AKR1C subfamily, namely, AKR1C1 (20α-HSD), AKR1C2 (type 3 3α-HSD), AKR1C3 (type 2 3α-HSD), and AKR1C4 (type 1 3α-HSD).[5] The four AKR1C isoforms share at least 84% sequence homology, while AKR1C1 and AKR1C2 in particular differ only by seven residues. Nonetheless, the four isoforms display distinct positional and stereo preferences with respect to their substrates and are involved in different physiological roles.[6] The functional plasticity of the AKR1C isoforms highlights their ability to modulate levels of different steroid hormones such as androgens, estrogens, and progestins, and as such they are considered important targets for drug design.[7,8]

AKR1C1 has a major role in progesterone metabolism that is essential for the maintenance of pregnancy.[9] The conversion of progesterone to an inactive progestin, 20-hydroxyprogesterone, by AKR1C1 is associated with premature birth, leading to infant morbidity and mortality.[10,11] AKR1C1 also plays an important role in brain function, where it modulates the occupancy of γ-aminobutyric acid type A receptors through its 3α- and 20α-HSD activity.[12] AKR1C1 reduces neuroactive steroids (3α,5α-tetrahydroprogesterone and 5α-tetrahydrodeoxycorticosterone) and their precursors (5α-dihydroprogesterone and progesterone) to inactive 20α-hydroxysteroids, thereby removing them from the synthetic pathway.[13] The elimination of neuroactive steroids by AKR1C1 is implicated in symptoms of premenstrual syndrome and other neurological disorders.[14]

Scheme 1

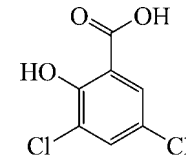

3,5-Dichlorosalicylic acid

Recent studies indicate that the enzyme is also involved in the development of several human and rodent tumors, such as lung, endometrial, esophageal, ovarian, and breast cancers, and suggests that its overexpression in cancer cells is also related to drug-resistance against several anticancer agents.[15–19] Thus the discovery of specific inhibitors for AKR1C1 offers an attractive strategy for the development of new therapeutic agents.

Recently, inhibitors of AKR1C1 were identified from a virtual screening-based study, of which 3,5-diiodosalicylic acid was reported to be the most potent competitive inhibitor of the enzyme with a K_i value in the sub-μM range.[20] Here we report the first structure of AKR1C1 in ternary complex with coenzyme and 3,5-dichlorosalicylic acid, an analogue of 3,5-diiodosalicylic acid discovered from a similarity search and found to be a more potent competitive inhibitor of AKR1C1, displaying a K_i value of 5.9 nM. In an effort to further characterize the inhibitor-binding site, we have compared the structures of the active-sites for the four AKR1C isoforms and used site-directed mutagenesis coupled with inhibitor binding studies to identify the role of several key residues in inhibitor binding and selectivity to the AKR1C isoforms in general and to AKR1C1 in particular. The results should facilitate the development of specific inhibitors of AKR1C1 with potential use in the treatments against cancer and premature birth.

Results and Discussion

Structure of the Ternary Complex. The inhibitor 3,5-dichlorosalicylic acid (Scheme 1) was identified from a similarity search preformed on the recently reported AKR1C1 competitive inhibitor 3,5-diiodosalicylic acid[20] and its potency evaluated against the four AKR1C isoforms as described in the Experimental Section. The crystal structure of AKR1C1 in ternary complex with $NADP^+$ and the inhibitor was determined at 1.8 Å resolution, with a final R_{cryst} of 17.4% and R_{free} of 21.7%

† Protein Data Bank: ID code 3C3U.

* To whom correspondence should be addressed. Phone: 61-3-9903-9691. Fax: 61-3-9903-9582. E-mail: ossama.el-kabbani@vcp.monash.edu.au.

‡ Medicinal Chemistry and Drug Action, Monash Institute of Pharmaceutical Sciences.

§ Laboratory of Biochemistry, Gifu Pharmaceutical University.

|| Contributed equally to this work and share first authorship.

[a] Abbreviations: HSD, hydroxysteroid dehydrogenase; AKR1C1, 20α-hydroxysteroid dehydrogenase; AKR1C2, type 3 3α-hydroxysteroid dehydrogenase; AKR1C3, type 2 3α-hydroxysteroid dehydrogenase; AKR1C4, type 1 3α-hydroxysteroid dehydrogenase; *S*-tetralol, *S*-(+)-1,2,3,4-tetrahydro-1-naphthol; ALR1, aldehyde reductase; ALR2, aldose reductase.

10.1021/jm8003575 CCC: $40.75
Published on Web 07/12/2008

Table 1. Data Collection and Refinement Statistics

data collection and processing	
space group	$P2_1$
cell dimensions	$a = 39.36$ Å $b = 84.23$ Å $c = 49.18$ Å $\beta = 91.2°$
radiation source	rotating anode
wavelength (Å)	1.54178
diffraction data[a]	
resolution (Å)	30−1.8
number of observed reflections	82647 (6284)
number of unique reflections	26329 (2076)
redundancy	2.9 (2.7)
completeness (%)	96.3 (87.6)
$I/\sigma(I)$	11.5 (2.5)
R_{merge} (%)	5.0 (22.9)
refinement statistics	
resolution (Å)	30−1.8
protein residues	320
solvent molecules	328
zinc ion	1
cofactor	1
inhibitor	1
R_{free} (%)	21.7
R_{cryst} (%)	17.4
root mean square deviations	
bonds (Å)	0.017
angles (deg)	1.5
Ramachandran plot	
residues in most favored regions (%)	93%
residues in allowed regions (%)	6.7%
estimated coordinated error	
Luzzati mean coordinate error (Å)	0.195
mean B factors (Å^2)	
protein	22.3
$NADP^+$	19.3
inhibitor	22.9
zinc ion	23.3

[a] Statistics for the highest resolution shell (1.86−1.80 Å) are shown within parentheses.

(Table 1). The backbone dihedral angles of 93% and 6.7% of the residues were in the most favored and allowed regions, respectively, in the Ramachandran plot. Only Ser221, which lies adjacent to the active site residue His222, that is involved in a hydrogen bonding interaction with the inhibitor, was found in the disallowed region due to a short contact with the coenzyme through its main chain. During the refinement process, double conformations were assigned to the following five residues Leu35, Ile49, Cys242, Ser290, and Ser320. There was one monomer per asymmetric unit and an estimated 44.2% solvent content occupying the unit cell volume.[21] The final model consisted of 320 amino acid residues, missing the first three N-terminal residues due to lack of corresponding electron density, 328 solvent molecules, one $NADP^+$ molecule, one inhibitor molecule, and a zinc ion from the crystallization buffer. The zinc ion was present in coordination with a water molecule, the side-chain of Glu133, and the side-chains of Glu292 and His248 from the neighboring symmetry-related molecule. A summary of the refinement statistics for the geometry and stereochemistry of the final model is provided in Table 1.

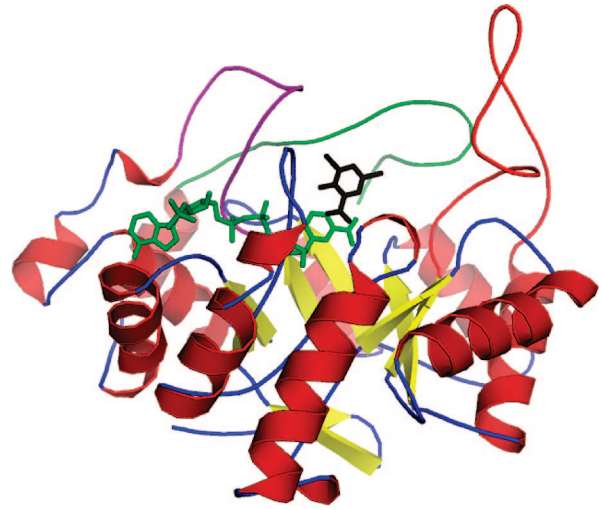

Figure 1. Schematic representation of the overall structure of the ternary complex. The α-helices are shown in red and the β-sheets are in yellow. The three main loops that interact with the inhibitor (black) and coenzyme (green) are loops A (residues 117−143), B (residues 217−234), and C (residues 299−323) shown at the top in red, purple, and green, respectively.

The structure of AKR1C1 is comprised of an eight-stranded α/β-barrel with the $NADP^+$ bound in an extended conformation adjacent to an active site located at the C-terminal end of the barrel (Figure 1). Well-defined electron density observed for the inhibitor molecule allowed unambiguous fitting of 3,5-dicholorosalicylic acid with its hydroxyl group pointing toward His222. The inhibitor-binding pocket is lined by side chains contributed by the 11 amino acid residues Tyr24, Leu54, Tyr55, Trp86, His117, His222, Glu224, Trp227, Leu306, Leu308, and Phe311. The inhibitor molecule is anchored from its carboxylate group that forms hydrogen bonds with the catalytic residues His117 (2.8 Å) and Tyr55 (3.1 Å), while the hydroxyl group is hydrogen bonded to His222 (2.8 Å). The structure of the AKR1C1 inhibitor-binding site is shown in stereo in Figure 2.

Selectivity Determinants of Inhibitor Binding. Analysis of the inhibitor binding site revealed four nonconserved residues (Leu54, His222, Leu306, and Leu308) in the human AKR1C isoforms that are present within van der Waals contacts (<4.0 Å) from the inhibitor and thus should be considered when designing specific inhibitors of AKR1C1. Superposition of the structures of AKR1C1, AKR1C2 (PDB code 1IHI), AKR1C3 (PDB code 1RYO) and AKR1C4 (PDB code 2FVL) is shown in Figure 3. The His222Ser mutation in AKR1C1 resulted in a reduction in the potency of 3,5-dicholorosalicylic acid (Table 2). This residue is present at the N-terminal end of loop B that undergoes an induced fit during the binding of coenzyme,[22] and the effect of the mutation suggests that the hydrogen bond plays a role in binding the inhibitor in the proper orientation. Additionally, the replacement of His222 in AKR1C1 with Gln in AKR1C3 and AKR1C4 is likely to maintain the hydrogen bonding interaction between this residue and the inhibitor. In the inhibitor binding site, AKR1C1 and AKR1C2 differ only by one amino acid residue, which is Leu54 in AKR1C1 and is Val54 in AKR1C2 (Figure 3). While the effect of the Leu54Val mutation on the 3,5-dicholorosalicylic acid inhibition was small, it is not surprising that this mutation made the inhibition of AKR1C1 more similar to that of AKR1C2 (Table 2). It is noteworthy that the importance of the bulky side chain of Leu54 in AKR1C1 in dictating the binding

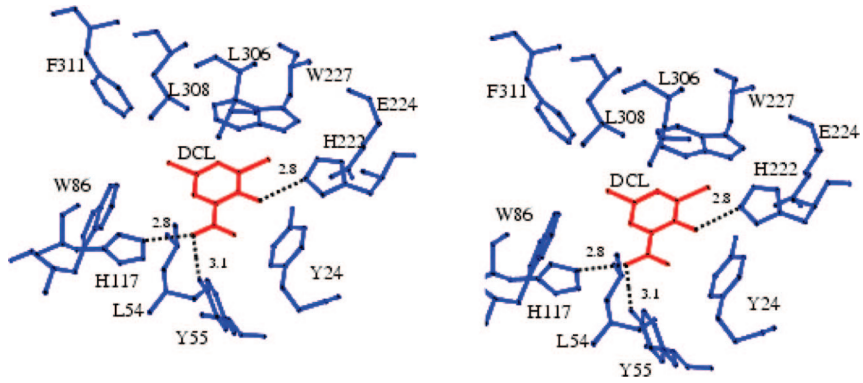

Figure 2. Stereo view of 3,5-dichlorosalicylic acid bound in the active site of AKR1C1. The inhibitor (DCL) is shown in red, and the surrounding residues are labeled with their single letter code for clarity and shown in blue. The hydrogen bonds are shown as black dotted lines with corresponding distances given in angstroms.

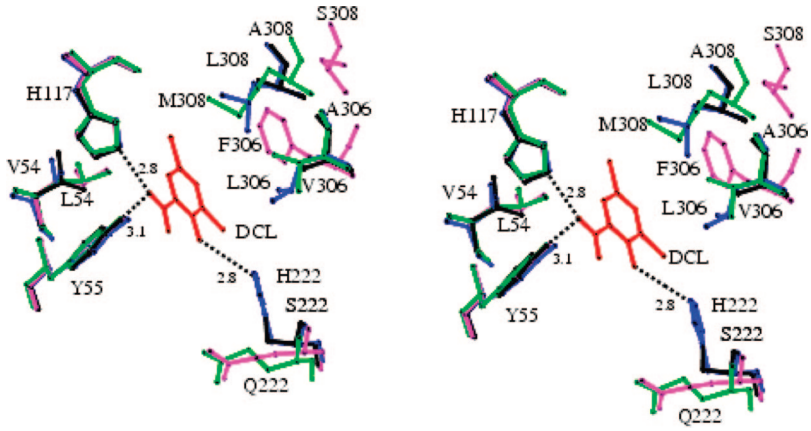

Figure 3. Comparison of the nonconserved inhibitor-binding residues in the active sites of the human AKR1C isoforms. The modeled mutant residues (Leu54Val, His222Ser, Leu306Ala, and Leu308Ala) in AKR1C1 (black) and the corresponding residues in AKR1C2 (blue), AKR1C3 (purple), AKR1C4 (green), and 3,5-dichlorosalicylic acid (red) are shown in their respective colors. The conserved catalytic residues Tyr55 and His117 are also included.

Table 2. K_i Values of 3,5-Dichlorosalicylic Acid for the Human AKR1C Isoforms (AKR1C1, AKR1C2, AKR1C3, and AKR1C4) and Mutant Forms of AKR1C1 (Leu54Val, His222Ser, Leu306Ala, and Leu308Ala)

K_i values (nM)[a]							
AKR1C1	Leu54Val	His222Ser	Leu306Ala	Leu308Ala	AKR1C2	AKR1C3	AKR1C4
5.9 ± 0.8	85 ± 7.6 (14)	58 ± 10 (10)	270 ± 29 (46)	2800 ± 300 (470)	70 ± 2.0 (12)	94000 ± 1300 (16000)	24000 ± 2100 (4100)

[a] The number of fold increase in K_i values relative to AKR1C1 is shown within parentheses.

confirmation of the steroidal substrate in the active site was pointed out in a previous study.[22]

The analysis of the crystal structure together with the results obtained from the mutagenesis indicated that the greater than 4000-fold difference in inhibitor potency between AKR1C1 and the two isoforms AKR1C3 and AKR1C4 is derived mainly from the nonconserved interactions between the inhibitor and residues from the C-terminal loop. Mutations of the nonconserved Leu306 (Phe in AKR1C3 and Val in AKR1C4) and Leu308 (Ser in AKR1C3 and Met in AKR1C4) to Ala residues in AKR1C1 resulted in significant increases in the K_i value for 3,5-dichlorosalicylic acid. Of the four corresponding residues in AKR1C3 and AKR1C4, only Met308 of AKR1C4 is present within van der Waals contacts of the modeled inhibitor (Figure 3). It should be noted that the role of Leu residues from the C-terminal loop of the AKR enzymes aldose reductase (ALR2) and aldehyde reductase (ALR1) in inhibitor binding and selectivity has been thoroughly investigated.[23–25] Leu300 in ALR2 (Pro in ALR1) accounts for the difference in inhibitor potency for the two enzymes and may undergo an induced fit upon inhibitor binding to ALR2. In the case of AKR1C1, there was no apparent induced fit upon the binding of 3,5-dichlorosalicylic acid to the enzyme compared to the ternary structure with bound 20α-hydroxyprogesterone.[22]

Experimental Section

Site-Directed Mutagenesis and Purification of Recombinant Enzymes. Mutagenesis was performed using a QuickChange site-directed mutagenesis kit (Stratagene) and pGEX-2T expression plasmid harboring cDNA for AKR1C1[26] as the template according to the protocol described by the manufacturer. The primer pair used for the mutagenesis was composed of sense and antisense oligonucleotides to alter a codon of AKR1C1 cDNA. The 29- to 30-mer primers were synthesized to give the His222Ser, Leu306Ala, and Leu308Ala mutant enzymes. The coding regions of the cDNAs in the expression plasmids were sequenced by using a Beckman CEQ2000XL DNA sequencer in order to confirm the presence of the desired mutation and ensure that no other mutation had occurred. The recombinant wild-type (WT) and mutant enzymes were expressed in *Escheri-*

chia coli JM109 and purified to homogeneity as previously described.[26] The Leu54Val mutant AKR1C1,[27] AKR1C2,[28] AKR1C3,[29] and AKR1C4[30] were also prepared and purified to homogeneity as previously described. Protein concentration was determined by a bicinchoninic acid protein assay reagent kit (Pierce) using bovine serum albumin as the standard.

Assay of Enzyme Activity. The activity was assayed by measuring the rate of change in NADPH fluorescence (at 455 nm with an excitation wavelength of 340 nm) at 298 K. The reaction mixture consisted of 0.1 M potassium phosphate buffer, pH 7.4, 0.25 mM $NADP^+$, *S*-(+)-1,2,3,4-tetrahydro-1-naphthol (*S*-tetralol), and enzyme, in a total volume of 2.0 mL. The inhibitor was dissolved in methanol and added to the reaction mixture in which the final concentration of methanol was less than 2.5%. When the fluorescence due to the high concentration of inhibitor interfered with the fluorometric assay, the enzyme activity was determined by measuring the rate of change in NADPH absorbance at 340 nm. The inhibitor constant, K_i, was determined from a Lineweaver−Burk plot using five concentrations of substrate, 5β-pregnane-3α,20α-diol (for AKR1C1) or *S*-tetralol (for the other enzymes), and is expressed as the mean ± standard error of at least three determinations.

Crystallization. Before crystallization, AKR1C1 at 21 mg/mL in 50 mM Tris-HCl buffer (pH 8.5) and 5 mM 2-mercaptoethanol was mixed with $NADP^+$ and inhibitor (molar ratio of AKR1C1: $NADP^+$:inhibitor was 1:3:3). The ternary complex was crystallized using the vapor diffusion method. The AKR1C1/$NADP^+$/inhibitor solution was mixed with an equal volume of the crystallization buffer (25% (v/v) polyethylene glycol monomethyl ether 550, 0.02 M zinc sulfate in 0.1 M MES buffer (pH 6.5)), and 10 μL hanging droplets were placed above a well solution (1 mL) containing the crystallization buffer. Rectangular crystals appeared at 295 K within one week and grew to maximum dimensions of 0.3 mm × 0.1 mm × 0.05 mm. The inhibitor 3,5-dichlorosalicylic acid with 97% purity was obtained from the Sigma-Aldrich Chemical Co.

X-Ray Data Collection and Structural Determination. The AKR1C1 ternary complex crystal was briefly soaked in the crystallization buffer (0.1 M MES pH 6.5, 0.01 M zinc sulfate, 25% (v/v) polyglycol monomethylether 550) containing 2% (v/v) inhibitor plus 25% (v/v) glycerol for cryoprotection). The diffraction data were collected at a temperature of 100 K on a MAR-345 image plate system mounted on a Rigaku RU300 rotating anode generator operating at 50 kV and 100 mA. X-ray diffraction data were collected up to 1.8 Å resolution and processed with HKL2000 and SCALEPACK.[31] Exposure time (10 min), oscillation range (1°), and crystal−detector distance (140 mm) were adjusted to optimize data collection, allowing the measurement of 160° in reciprocal space for a near complete data set. The structure was solved by the molecular replacement method using the program MOLREP in the CCP4 suite of crystallographic software[32] and the atomic coordinates of AKR1C1 as the search model (PDB code 1MRQ).[22] The initial model was subjected to iterative cycles of manual fitting into $2F_o - F_c$ and $F_o - F_c$ electron density maps using Coot,[33] followed by structural refinement using REFMAC.[34] The inhibitor molecule, water, and zinc ion were added towards the end of the refinement. Data collection and refinement statistics are summarized in Table 1. Stereodiagrams were prepared using MOLSCRIPT.[35]

Acknowledgment. We thank Dr. Roland Chung for his assistance with the data collection experiment. The research project was supported by an Australian Research Council Linkage International Award (O.E. & A.H.). U.D. is the recipient of a Monash Graduate School postgraduate scholarship.

References

(1) Penning, T. M. Hydroxysteroid dehydrogenases and pre-receptor regulation of steroid hormone action. *Hum. Reprod. Update* **2003**, *9*, 193–205.
(2) Jez, J. M.; Bennett, M. J.; Schlegel, B. P.; Lewis, M.; Penning, T. M. Comparative anatomy of the aldo-keto reductase superfamily. *Biochem. J.* **1997**, *326*, 625–636.
(3) Jez, J. M.; Penning, T. M. The aldo-keto reductase (AKR) superfamily: an update. *Chem. Biol. Interact.* **2001**, *130−132*, 499–525.
(4) Oppermann, U.; Filling, C.; Hult, M.; Shafqat, N.; Wu, X.; Lindh, M.; Shafqat, J.; Nordling, E.; Kallberg, Y.; Persson, B.; Jornvall, H. Short-chain dehydrogenases/reductases (SDR): the 2002 update. *Chem.−Biol. Interact.* **2003**, *143−144*, 247–253.
(5) Penning, T. M.; Bennett, M. J.; Smith-Hoog, S.; Schlegel, B. P.; Jez, J. M.; Lewis, M. Structure and function of 3α-hydroxysteroid dehydrogenase. *Steroids* **1997**, *62*, 101–111.
(6) Penning, T. M.; Burczynski, M. E.; Jez, J. M.; Hung, C. F.; Lin, H. K.; Ma, H.; Moore, M.; Palackal, N.; Ratnam, K. Human 3α-hydroxysteroid dehydrogenase isoforms (AKR1C1−AKR1C4) of the aldo-keto reductase superfamily: functional plasticity and tissue distribution reveals roles in the inactivation and formation of male and female sex hormones. *Biochem. J.* **2000**, *351*, 67–77.
(7) Penning, T. M.; Jin, Y.; Steckelbroeck, S.; Lanisnik Rizner, T.; Lewis, M. Structure−function of human 3α-hydroxysteroid dehydrogenases: genes and proteins. *Mol. Cell. Endocrinol.* **2004**, *215*, 63–72.
(8) Bauman, D. R.; Steckelbroeck, S.; Penning, T. M. The roles of aldo-keto reductases in steroid hormone action. *Drug News Perspect.* **2004**, *17*, 563–578.
(9) Zhang, Y.; Dufort, I.; Rheault, P.; Luu-The, V. Characterization of a human 20α-hydroxysteroid dehydrogenase. *J. Mol. Endocrinol.* **2000**, *25*, 221–228.
(10) Lewis, M. J.; Wiebe, J. P.; Heathcote, J. G. Expression of progesterone metabolizing enzyme genes (AKR1C1, AKR1C2, AKR1C3, SRD5A1, SRD5A2) is altered in human breast carcinoma. *BMC Cancer* **2004**, *4*, 27–39.
(11) Piekorz, R. P.; Gingras, S.; Hoffmeyer, A.; Ihle, J. N.; Weinstein, Y. Regulation of progesterone levels during pregnancy and parturition by signal transducer and activator of transcription 5 and 20α-hydroxysteroid dehydrogenase. *Mol. Endocrinol.* **2005**, *19*, 431–440.
(12) Lambert, J. J.; Belelli, D.; Hill-Venning, C.; Peters, J. A. Neurosteroids and $GABA_A$ receptor function. *Trends Pharmacol. Sci.* **1995**, *16*, 295–303.
(13) Higaki, Y.; Usami, N.; Shintani, S.; Ishikura, S.; El-Kabbani, O.; Hara, A. Selective and potent inhibitors of human 20α-hydroxysteroid dehydrogenase (AKR1C1) that metabolizes neurosteroids derived from progesterone. *Chem. Biol. Interact.* **2003**, *143−144*, 503–513.
(14) Eser, D.; Schüle, C.; Baghai, T. C.; Romeo, E.; Uzunov, D. P.; Rupprecht, R. Neuroactive steroids and affective disorders. *Pharmacol., Biochem. Behav.* **2006**, *84*, 656–666.
(15) Wiebe, J. P. Role of progesterone metabolites in mammary cancer. *J. Dairy Res.* **2005**, *72*, 51–57.
(16) Deng, H. B.; Adikari, M.; Parekh, H. K.; Simpkins, H. Ubiquitous induction of resistance to platinum drugs in human ovarian, cervical, germ−cell and lung carcinoma tumor cells overexpressing isoforms 1 and 2 of dihydrodiol dehydrogenase. *Cancer Chemother. Pharmacol.* **2004**, *54*, 301–307.
(17) Wang, H. W.; Lin, C. P.; Chiu, J. H.; Chow, K. C.; Kuo, K. T.; Lin, C. S.; Wang, L. S. Reversal of inflammation-associated dihydrodiol dehydrogenases (AKR1C1 and AKR1C2) overexpression and drug resistance in nonsmall cell lung cancer cells by wogonin and chrysin. *Int. J. Cancer* **2007**, *120*, 2019–2027.
(18) Rizner, T. L.; Smuc, T.; Rupreht, R.; Sinkovec, J.; Penning, T. M. AKR1C1 and AKR1C3 may determine progesterone and estrogen ratios in endometrial cancer. *Mol. Cell. Endocrinol.* **2006**, *248*, 126–135.
(19) Selga, E.; Noé, V.; Ciudad, C. J. Transcriptional regulation of aldo-keto reductase 1C1 in HT29 human colon cancer cells resistant to methotrexate: role in the cell cycle and apoptosis. *Biochem. Pharmacol.* **2008**, *75*, 414–426.
(20) Dhagat, U.; Carbone, V.; Chung, R. P.; Matsunaga, T.; Endo, S.; Hara, A.; El-Kabbani, O. A salicylic acid-based analogue discovered from virtual screening as a potent inhibitor of human 20α-hydroxysteroid dehydrogenase. *Med. Chem.* **2007**, *3*, 546–50.
(21) Matthews, B. W. Solvent content of protein crystals. *J. Mol. Biol.* **1968**, *33*, 491–497.
(22) Couture, J. F.; Legrand, P.; Cantin, L.; Luu-The, V.; Labrie, F.; Breton, R. Human 20α-hydroxysteroid dehydrogenase: crystallographic and site-directed mutagenesis studies lead to the identification of an alternative binding site for C21-steroids. *J. Mol. Biol.* **2003**, *331*, 593–604.
(23) El-Kabbani, O.; Podjarny, A. Selectivity determinants of the aldose reductase and aldehyde reductase inhibitor binding sites. *Cell. Mol. Life Sci.* **2007**, *64*, 1970–1978.
(24) El-Kabbani, O.; Carbone, V.; Darmanin, C.; Oka, M.; Mitschler, A.; Podjarny, A.; Schulze-Briese, C.; Chung, R. P.-T. Structure of aldehyde reductase holoenzyme in complex with the potent aldose reductase inhibitor fidarestat: implications for inhibitor binding and selectivity. *J. Med. Chem.* **2005**, *48*, 5536–5542.

(25) Petrova, T.; Steuber, H.; Hazemann, I.; Cousido-Siah, A.; Mitschler, A.; Chung, R. P.-T.; Oka, M.; Klebe, G.; El-Kabbani, O.; Joachimiak, A.; Podjarny, A. Factorizing selectivity determinants of inhibitor binding towards aldose and aldehyde reductases: structural and thermodynamic properties of the aldose reductase mutant Leu300Pro/Fidarestat complex. *J. Med. Chem.* **2005**, *48*, 5659–5665.

(26) Matsuura, K.; Hara, A.; Deyashiki, Y.; Iwasa, H.; Kume, T.; Ishikura, S.; Shiraishi, H.; Katagiri, Y. Roles of the C-terminal domains of human dihydrodiol dehydrogenase isoforms in the binding of substrates and modulators: probing with chimaeric enzymes. *Biochem. J.* **1998**, *336*, 429–436.

(27) Matsuura, K.; Deyashiki, Y.; Sato, K.; Ishida, N.; Miwa, G.; Hara, A. Identification of amino acid residues responsible for differences in substrate specificity and inhibitor sensitivity between two human liver dihydrodiol dehydrogenase isoenzymes by site-directed mutagenesis. *Biochem. J.* **1997**, *323*, 61–64.

(28) Shiraishi, H.; Ishikura, S.; Matsuura, K.; Deyashiki, Y.; Ninomiya, M.; Sakai, S.; Hara, A. Sequence of the cDNA of a human dihydrodiol dehydrogenase isoform (AKR1C2) and tissue distribution of its mRNA. *Biochem. J.* **1998**, *334*, 399–405.

(29) Matsuura, K.; Shiraishi, H.; Hara, A.; Sato, K.; Deyashiki, Y.; Ninomiya, M.; Sakai, S. Identification of a principal mRNA species for human 3α-hydroxysteroid dehydrogenase isoform (AKR1C3) that exhibits high prostaglandin D_2 11-ketoreductase activity. *J. Biochem.* **1998**, *124*, 940–946.

(30) Deyashiki, Y.; Tamada, Y.; Miyabe, Y.; Nakanishi, M.; Matsuura, K.; Hara, A. Expression and kinetics properties of a recombinant 3α-hydroxysteroid/dihydrodiol dehydrogenase isoenzyme of human liver. *J. Biochem.* **1995**, *118*, 285–290.

(31) Otwinowski, Z.; Minor, W. Processing of X-ray diffraction data collected in oscillation mode. *Methods Enzymol.* **1997**, *276*, 307–326.

(32) Collaborative Computational Project, N. The CCP4 suite: programs for protein crystallography. *Acta Crystallogr., Sect. D: Biol. Crystallogr.* **1994**, *50*, 760–763.

(33) Emsley, P.; Cowtan, K. Coot: model-building tools for molecular graphics. *Acta Crystallogr., Sect. D: Biol. Crystallogr.* **2004**, *60*, 2126–2132.

(34) Murshudov, G. N.; Vagin, A. A.; Dodson, E. J. Refinement of macromolecular structures by the maximum-likelihood method. *Acta Crystallogr., Sect. D: Biol. Crystallogr.* **1997**, *53*, 240–255.

(35) Kraulis, P. MOLSCRIPT: a program to produce both detailed and schematic plots of protein structures. *J. Appl. Crystallogr.* **1991**, *24*, 946–950.

JM8003575